Accepted Manuscript

Analytical solution for buckling of mindlin plates subjected to arbitrary boundary conditions

Eugenio Ruocco , Vincenzo Mallardo , Vincenzo Minutolo , Danilo Di Giacinto

PII: S0307-904X(17)30392-X
DOI: 10.1016/j.apm.2017.05.052
Reference: APM 11804

To appear in: *Applied Mathematical Modelling*

Received date: 14 April 2016
Revised date: 5 April 2017
Accepted date: 25 May 2017

Highlights

- We investigate the buckling of Mindin plates through the extended Kantorovich method.
- The approach allows an analytical solution without any hypothesis on the Boundary Conditions.
- The effect of pure shear loads is taken into account.
- The nonlinear strain-displacement terms neglected under Von Karman hypothesis are evaluated.

ANALYTICAL SOLUTION FOR BUCKLING OF MINDLIN PLATES SUBJECTED TO ARBITRARY BOUNDARY CONDITIONS

Eugenio Ruocco, Vincenzo Mallardo, Vincenzo Minutolo and Danilo Di Giacinto

DICDEA, Department of Ingegneria Civile, Design, Edilizia e Ambiente, University of Campania "Luigi Vanvitelli"
e-mail: eugenio.ruocco@unicampania.it

Keywords: Plate stability; First order plate theory; Extended Kantorovich method; General boundary conditions; Closed-form solution; Levy-type solution.

Abstract. *The study investigates buckling behavior of isotropic plates subjected to axial, biaxial and pure shear loads. The effect of transverse shear deformation is taken into account by adopting the Mindlin first order shear theory. By applying the extended Kantorovich method, an exact solution is presented without any approximation on the boundary conditions. The procedure is proposed at thin, moderately thick and thick isotropic plates. The obtained results are in good agreement with those available in literature and they demonstrate the accuracy of the proposed procedure.*

1 INTRODUCTION

For more than a century, researchers in structural mechanics have been attempting to obtain reliable analytical results for the buckling response of rectangular plates in terms of critical load and corresponding critical mode [1]. However, most of the analytical solutions that are available in literature deals with plates simply supported on two opposite edges, whereas on the remainder borders can be supported, clamped or present any mixed boundary condition as well. In such a context an extensive literature has been developed to the exact buckling analysis of thin plates, on the basis of the Kirchhoff plate theory (e.g. see Refs [2-4]).

Although with less frequency, also thick plates, as described by Mindlin [5] or third-order [6] shear deformation theories received researcher's attention. Some results can be found in the work of Sayyad and Ghugal [7] where a Navier type analytical solution, based on a novel trigonometric shear and normal deformation theory, for the buckling of simply supported rectangular isotropic, transversely isotropic or orthotropic plates were proposed. Furthermore, Hong *et al.* [8] solved analytically the buckling problem of thick circular plates under uniform radial loads; Wang *et al.* [9] presented generic buckling solutions for isotropic in-plane loaded Mindlin plates of regular, polygonal, elliptical, and annular shape.

Most of the closed form solutions proposed in literature was obtained by assuming that the solution is separable, i.e. the generalized displacement $\mathbf{s}(x, y)$ governing the kinematical model can be uncoupled with respect to the coordinates defined on the middle plane of the plate by the following product:

$$\mathbf{s}(x, y) = \mathbf{s}_1(x) \cdot \mathbf{s}_2(y)$$

where, accordingly to the Mindlin's kinematical hypothesis, $\mathbf{s}(x,y)=\left[s_z(x,y)\ \theta_x(x,y)\ \ \theta_y(x,y)\right]^T$ collects the out-of-plane displacement and the rotations around the x and y axes and $\mathbf{s}_1(x)$ and $\mathbf{s}_2(y)$ are suitable functions. For instance, the Levy type solution method assumes an approximate solution of the type $\mathbf{s}_1(x)=\left[\sin\xi,\,\cos\xi,\,\sin\xi\right]^T$, where $\xi=m\pi x/a$, m and a are the number of half-waves in x direction and the x-size of the plate, respectively. Such a decomposition allows a decoupling of the Partial Differential Equations (PDE) of equilibrium, resulting into a set of ordinary differential equations (ODE) in term of the one dimensional unknown functions $\mathbf{s}_2(y)=\left[w(y)\ \ \varphi_x(y)\ \ \varphi_y(y)\right]$.

Finally, since the displacement $\mathbf{s}_1(x)$ automatically satisfies the simply supported boundary conditions on the two opposite sides parallel to the y-axes, such a solution is commonly reported as "exact" for simply supported plates.

Starting by the work of Liew *at al.* [10], this approximation was adopted by Xiang and Wei [11] to study buckling and vibration of stepped rectangular Mindlin plates and by Hosseini Ashemi and Arsanjani [12] the parametric analyses of rectangular plates with six different combinations of boundary condition. In such a context, the study of the effect of nonlinear strain components on the buckling response of isotropic and orthotropic Mindlin plates is investigated in [13] and [14]. Analytical solution can be found on axisymmetric plates by adopting a curvilinear coordinate system: in such a context, new analytical solution based on the first order shear theory and on the perturbation technique is presented for the axisymmetric buckling analysis of annular plates in [15]. Analytical solution for buckling of functional graded material truncated conical shells reinforced by orthogonal stiffeners is recently proposed in [16]. An analytical solution for the buckling and free vibration analysis of laminated beams by using a generalized high order shear deformation theory, derived by employing a Ritz solution to approximate the displacement field and Lagrange multipliers to consider the boundary conditions is reported in [17]. A Levy solution for determining analytical solutions for the bending, buckling and vibration of refined plate theory is reported in [18] C1

By the aforementioned research it results that adopting trigonometric description for $\mathbf{s}_1(x)$, as suggested by Levy type method, prevents to fulfill boundary conditions where derivatives of the displacement vanishes rather than the displacement itself. Moreover choosing a simple scalar for representing the displacement variation in the x-direction returns an intrinsically one-dimensional model, that is not capable to describe the buckling of a two-dimensional structure since it assumes *ab initio* that critical loads associated with more complex, or mixed, modes do not exist [19-20].

Motivated by the above issues, the present paper intends to introduce an enriched displacement field that, while maintaining the same advantages of the classical Levy type approach, overcomes the discussed limits and allows analytical solution of fully two-dimensional structure. The procedure is able to handle different boundary conditions on any side of the plate and different in-plane loading, comprising non-uniform and shear ones. In order to show the effectiveness of the proposed approach, examples concerning biaxial tensile and compressive loads in the presence of piecewise clamped and partially supported sides have been reported and discussed.

2 GOVERNING EQUATIONS

Let us consider a rectangular, homogeneous plate of length *a*, width *b* and uniform thickness *h*. The material constituting the plate is linearly elastic, with modulus of elasticity *E*, Poisson's ratio ν and shear modulus $G = E/2(1+\nu)$. The coordinate system is taken in order to let the *x*-*y* plane coincides with the middle plane, the *z*-axis to be orthogonal to it and the origin of the coordinate system to be located at the center of the plate (Figure 1).

Different conditions concerning displacement and rotation can be imposed on the plate boundary, moreover in plane load for unit length can be prescribed as well along the middle plane borders. The load is described by means of normal, say N_x, N_y and tangent, say N_{xy}, components applied to the edges and collected into a vector $\mathbf{N} = \left(N_x, N_y, N_{xy}\right)$.

According to the Mindlin plate theory, the following representation of displacement is adopted:

$$\begin{aligned} \bar{u}(x,y,z) &= -z \cdot \varphi_x(x,y) \\ \bar{v}(x,y,z) &= -z \cdot \varphi_y(x,y) \\ \bar{w}(x,y,z) &= w(x,y) \end{aligned} \tag{1}$$

where $\bar{u}$, $\bar{v}$, $\bar{w}$ are the displacement components along the x, y, z axes, w is the displacement in the *z*-direction of a point on the middle plane, and (φ_x, φ_y) are the rotations around the *y*- and the *x*-axes respectively.

The strain-displacement equation has the following representation:

$$\begin{aligned} \varepsilon_x &= \bar{u}_{,x} + \frac{1}{2}\left(k_1 \bar{u}_{,x}^2 + k_2 \bar{v}_{,x}^2 + \bar{w}_{,x}^2\right) \\ \varepsilon_y &= \bar{v}_{,y} + \frac{1}{2}\left(k_1 \bar{u}_{,y}^2 + k_2 \bar{v}_{,y}^2 + \bar{w}_{,y}^2\right) \\ \gamma_{xy} &= \bar{u}_{,y} + \bar{v}_{,x} + k_1 \bar{u}_{,x}\bar{u}_{,y} + k_2 \bar{v}_{,x}\bar{v}_{,y} + \bar{w}_{,x}\bar{w}_{,y} \end{aligned} \tag{2}$$

where $(\varepsilon_x, \varepsilon_y)$ are the axial strains along the coordinates directions and γ_{xy} is the engineering shear strain. In Eqns. (2) the two coefficients k_1 and k_2 allow us to consider within only one equation two different models for the non-linear strain terms. Indeed, by setting $k_1 = k_2 = 0$ equation (2) restitutes the so-called von Kàrmàn model, where only out-of-plane second order displacement derivative is considered. Otherwise, by posing $k_1 = k_2 = 1$ the Koiter-Sanders model, based on the Green-Lagrange strain-displacement relations, can be obtained. The effect of such contributes, usually neglected in literature under the von Kàrmàn hypothesis, will be discussed in detail in the following.

In order to derive the non-linear equilibrium equations, the principle of stationary potential energy is used. The criterion, particularized by considering the generalized displacement reported in eq. (1), returns the following equilibrium equations:

$$\begin{aligned}
&-\kappa Gh\left(\left(\varphi_x - w,_x\right),_x + \left(\varphi_y - w,_y\right),_y\right) + N_x w,_{xx} + 2N_{xy} w,_{xy} + N_y w,_{yy} = 0 \\
&D\left(\left(\varphi_x,_x + \nu\varphi_y,_y\right),_x + \frac{1-\nu}{2}\left(\varphi_x,_y + \varphi_y,_x\right),_y\right) - \kappa Gh\left(\varphi_x - w,_x\right) + k_1 \frac{h^2}{12}\left(N_x \varphi_x,_{xx} + 2N_{xy}\varphi_x,_{xy} + N_y \varphi_x,_{yy}\right) = 0 \\
&D\left(\left(\varphi_y,_y + \nu\varphi_x,_x\right),_y + \frac{1-\nu}{2}\left(\varphi_x,_y + \varphi_y,_x\right),_x\right) - \kappa Gh\left(\varphi_y - w,_y\right) + k_2 \frac{h^2}{12}\left(N_x \varphi_y,_{xx} + 2N_{xy}\varphi_y,_{xy} + N_y \varphi_y,_{yy}\right) = 0
\end{aligned} \tag{3}$$

where κ is the shear correction factor.

Assuming $k_1 = k_2 = 0$ Eqns. (3), reduce to the classical Mindlin equations. Converseley, considering $k_1 = k_2 = 1$ the last two equations in (3) present new additional terms, usually neglected by the von Kàrmàn model that multiply the square of the thickness *h* and depending on the second derivative of the rotations.

A closed-form solution of the system (3) can be obtained by choosing the following uncoupled form of the displacement field:

$$\begin{aligned}
w(x,y) &= \mathbf{n}(x)\cdot\mathbf{w}(y) \\
\varphi_x(x,y) &= \mathbf{n}(x)\cdot\boldsymbol{\varphi}_x(y) \\
\varphi_y(x,y) &= \mathbf{n}(x)\cdot\boldsymbol{\varphi}_y(y)
\end{aligned} \tag{4}$$

where:

$$\mathbf{n}(x) = \left[\sin\xi \quad \cos\xi \quad \xi/m\pi \quad 1\right] \tag{5}$$

collects known, prescribed functions and:

$$\begin{aligned}
\mathbf{w}(y) &= \left[w_1(y) \quad w_2(y) \quad w_3(y) \quad w_4(y)\right]^T \\
\boldsymbol{\varphi}_x(y) &= \left[\varphi_{x1}(y) \quad \varphi_{x2}(y) \quad \varphi_{x3}(y) \quad \varphi_{x4}(y)\right]^T \\
\boldsymbol{\varphi}_y(y) &= \left[\varphi_{y1}(y) \quad \varphi_{y2}(y) \quad \varphi_{y3}(y) \quad \varphi_{y4}(y)\right]^T
\end{aligned} \tag{6}$$

are twelve unknown functions to be determined by solving the equations (3). A scheme of the out-of-plane displacement *w* is depicted in Figure 2.

The main difference between the present approach and the Levy type formulation available in literature consists in the fact that the vector **n**, that plays the role of a shape function, is usually a scalar function cointaining only the sinus term $\sin\xi$, whereas here is a vector function containing also cosine, linear and constant components. The consequence of this representation is that the displacement *w* is governed not only by the Levy type component w_1 represented in Figure 2a, but its description is enriched by the new terms reported in fig. 2b-d. Analogous consideration holds for the rotation components.

The buclking analysis requires the introduction of a common intensity parameter N_L and of three coefficients (α,β,γ) such that the in-plane compressive loads can be represented as:

$$N_x = -\alpha N_L;\quad N_y = -\beta N_L;\quad N_{xy} = -\gamma N_L \tag{7}$$

Substituting Eqns. (5-7) into Eqn. (3), the following sets of equations are finally obtained:

$$\begin{aligned}
&\sin\xi x\left[\left(\kappa Gh-\beta N_L\right)w_{1,yy}-\xi^2\left(\kappa Gh-\alpha N_L\right)w_1-\kappa Gh\,\varphi_{y1,y}+2\xi\gamma N_L w_{2,y}+\xi\kappa Gh\,\varphi_{x1}\right]+\\
&\cos\xi x\left[\left(\kappa Gh-\beta N_L\right)w_{2,yy}-\xi^2\left(\kappa Gh-\alpha N_L\right)w_2-\kappa Gh\,\varphi_{y2,y}-2\xi\gamma N_L w_{1,y}-\xi\kappa Gh\,\varphi_{x2}\right]+\\
&\frac{x}{a}\left[\left(\kappa Gh-\beta N_L\right)w_{3,yy}-\kappa Gh\,\varphi_{y3,y}\right]+\\
&\left[\left(\kappa Gh-\beta N_L\right)w_{4,yy}-\kappa Gh\varphi_{y4,y}-a^{-1}\left(\kappa Gh\varphi_{x4}+2\gamma N_L w_{3,y}\right)\right]=0
\end{aligned} \tag{8a}$$

$$\begin{aligned}
&\sin\xi x\left[\left(\frac{1-\nu}{2}D-\beta_1 N_L\right)\varphi_{x2,yy}-\left(\kappa Gh+\xi^2\left(D-\alpha_1 N_L\right)\right)\varphi_{x2}-\xi\kappa Gh\,w_2+2\xi\gamma_1 N_L\varphi_{x1,y}-\xi\frac{1+\nu}{2}D\varphi_{y2,y}\right]+\\
&\cos\xi x\left[\left(\frac{1-\nu}{2}D-\beta_1 N_L\right)\varphi_{x1,yy}-\left(\kappa Gh+\xi^2\left(D-\alpha_1 N_L\right)\right)\varphi_{x1}+\xi\kappa Gh\,w_1-2\xi\gamma_1 N_L\varphi_{x2,y}+\xi\frac{1+\nu}{2}D\varphi_{y1,y}\right]+\\
&\frac{x}{a}\left[\left(\frac{1-\nu}{2}D-\beta_1 N_L\right)\varphi_{x4,yy}-\kappa Gh\varphi_{x4}\right]+\\
&\left[\left(\frac{1-\nu}{2}D-\beta_1 N_L\right)\varphi_{x3,yy}-\kappa Gh\varphi_{x3}+a^{-1}\left(\frac{1+\nu}{2}D\varphi_{y3,y}+\kappa Ghw_3-2\gamma_1 N_L\,\varphi_{x4,y}\right)\right]=0
\end{aligned} \tag{8b}$$

$$\begin{aligned}
&\sin\xi x\left[\left(D-\beta_2 N_L\right)\varphi_{y1,yy}-\left(\kappa Gh+\xi^2\left(D\frac{1-\nu}{2}-\alpha_2 N_L\right)\right)\varphi_{y1}+\kappa Gh\,w_{1,y}+2\xi\gamma_1 N_L\varphi_{y2,y}-\xi\frac{1+\nu}{2}D\,\varphi_{x1,y}\right]+\\
&\cos\xi x\left[\left(D-\beta_2 N_L\right)\varphi_{y2,yy}-\left(\kappa Gh+\xi^2\left(D\frac{1-\nu}{2}-\alpha_2 N_L\right)\right)\varphi_{y2}+\kappa Gh\,w_{2,y}-2\xi\gamma_1 N_L\varphi_{y1,y}+\xi\frac{1+\nu}{2}D\,\varphi_{x2,y}\right]+\\
&\frac{x}{a}\left[\left(D-\beta_2 N_L\right)\varphi_{y3,yy}+\kappa Gh\,w_{3,y}-\kappa Gh\,\varphi_{y3}\right]+\\
&\left[\left(D-\beta_2 N_L\right)\varphi_{y4,yy}+\kappa Gh\,w_{4,y}-\kappa Gh\,\varphi_{y4}+a^{-1}\left(D\frac{1+\nu}{2}\varphi_{x4,y}-2\gamma_2 N_L\varphi_{y3,y}\right)\right]=0
\end{aligned} \tag{8c}$$

where $(\alpha_i,\beta_i,\gamma_i)=k_i(\alpha,\beta,\gamma)h^2/12$. Eqns. (8) admit solutions for any ξ if and only if any equation in the square brackets are equal to zero.

The resulting set of equations presents the particularity to be decoupled into two independent set, the first one:

$$
\begin{aligned}
&\left(\kappa Gh-\beta N_L\right)w_{1,yy}-\xi^2\left(\kappa Gh-\alpha N_L\right)w_1-\kappa Gh\,\varphi_{y1,y}+2\xi\gamma N_L w_{2,y}+\xi\kappa Gh\,\varphi_{x1}=0\\
&\left(\kappa Gh-\beta N_L\right)w_{2,yy}-\xi^2\left(\kappa Gh-\alpha N_L\right)w_2-\kappa Gh\,\varphi_{y2,y}-2\xi\gamma N_L w_{1,y}-\xi\kappa Gh\,\varphi_{x2}=0\\
&\left(\frac{1-\nu}{2}D-\beta_1 N_L\right)\varphi_{x2,yy}-\left(\kappa Gh+\xi^2\left(D-\alpha_1 N_L\right)\right)\varphi_{x2}-\xi\kappa Gh\,w_2+2\xi\gamma_1 N_L\varphi_{x1,y}-\xi\frac{1+\nu}{2}D\varphi_{y2,y}=0\\
&\left(\frac{1-\nu}{2}D-\beta_1 N_L\right)\varphi_{x1,yy}-\left(\kappa Gh+\xi^2\left(D-\alpha_1 N_L\right)\right)\varphi_{x1}+\xi\kappa Gh\,w_1-2\xi\gamma_1 N_L\varphi_{x2,y}+\xi\frac{1+\nu}{2}D\varphi_{y1,y}=0\\
&\left(D-\beta_2 N_L\right)\varphi_{y1,yy}-\left(\kappa Gh+\xi^2\left(D\frac{1-\nu}{2}-\alpha_2 N_L\right)\right)\varphi_{y1}+\kappa Gh\,w_{1,y}+2\xi\gamma_1 N_L\varphi_{y2,y}-\xi\frac{1+\nu}{2}D\varphi_{x1,y}=0\\
&\left(D-\beta_2 N_L\right)\varphi_{y2,yy}-\left(\kappa Gh+\xi^2\left(D\frac{1-\nu}{2}-\alpha_2 N_L\right)\right)\varphi_{y2}+\kappa Gh\,w_{2,y}-2\xi\gamma_1 N_L\varphi_{y1,y}+\xi\frac{1+\nu}{2}D\varphi_{x2,y}=0
\end{aligned}
\tag{9}
$$

of six equations in the six unknowns $\left(w_1,\varphi_{x1},\varphi_{y1},w_2,\varphi_{x2},\varphi_{y2}\right)$, the second one:

$$
\begin{aligned}
&\left(\kappa Gh-\beta N_L\right)w_{3,yy}-\kappa Gh\,\varphi_{y3,y}=0\\
&\left(\kappa Gh-\beta N_L\right)w_{4,yy}-\kappa Gh\varphi_{y4,y}-a^{-1}\left(\kappa Gh\varphi_{x4}+2\gamma N_L w_{3,y}\right)=0\\
&\left(\frac{1-\nu}{2}D-\beta_1 N_L\right)\varphi_{x4,yy}-\kappa Gh\,\varphi_{x4}=0\\
&\left(\frac{1-\nu}{2}D-\beta_1 N_L\right)\varphi_{x3,yy}-\kappa Gh\varphi_{x3}+a^{-1}\left(\frac{1+\nu}{2}D\varphi_{y3,y}+\kappa Gh w_3-2\gamma_1 N_L\,\varphi_{x4,y}\right)=0\\
&\left(D-\beta_2 N_L\right)\varphi_{y3,yy}+\kappa Gh\,w_{3,y}-\kappa Gh\,\varphi_{y3}=0\\
&\left(D-\beta_2 N_L\right)\varphi_{y4,yy}+\kappa Gh\,w_{4,y}-\kappa Gh\,\varphi_{y4}+a^{-1}\left(D\frac{1+\nu}{2}\varphi_{x4,y}-2\gamma_2 N_L\varphi_{y3,y}\right)=0
\end{aligned}
\tag{10}
$$

of six equations in the six unknowns $\left(w_3,\varphi_{x3},\varphi_{y3},w_4,\varphi_{x4},\varphi_{y4}\right)$.

Since $N_{xy}=-\gamma N_L$, it is interesting to point out that both the system of equations can be further decoupled when the coefficient γ vanishes, that is when there is no shear load applied. In this case, one obtains four set of independent equations each of them corresponding to only one of the shape functions in **n**:

$$\begin{aligned}
&\left(\kappa Gh-\beta N_L\right)w_{1,yy}-\xi^2\left(\kappa Gh-\alpha N_L\right)w_1-\kappa Gh\varphi_{y1,y}+\xi\kappa Gh\varphi_{x1}=0\\
&\left(\frac{1-\nu}{2}D-\beta_1 N_L\right)\varphi_{x1,yy}-\left(\kappa Gh+\xi^2\left(D-\alpha_1 N_L\right)\right)\varphi_{x1}+\xi\kappa Gh w_1+\xi\frac{1+\nu}{2}D\varphi_{y1,y}=0\\
&\left(D-\beta_2 N_L\right)\varphi_{y1,yy}-\left(\kappa Gh+\xi^2\left(D\frac{1-\nu}{2}-\alpha_2 N_L\right)\right)\varphi_{y1}+\kappa Gh w_{1,y}-\xi\frac{1+\nu}{2}D\varphi_{x1,y}=0
\end{aligned} \tag{11a}$$

$$\begin{aligned}
&\left(\kappa Gh-\beta N_L\right)w_{2,yy}-\xi^2\left(\kappa Gh-\alpha N_L\right)w_2-\kappa Gh\varphi_{y2,y}-\xi\kappa Gh\varphi_{x2}=0\\
&\left(\frac{1-\nu}{2}D-\beta_1 N_L\right)\varphi_{x2,yy}-\left(\kappa Gh+\xi^2\left(D-\alpha_1 N_L\right)\right)\varphi_{x2}-\xi\kappa Gh w_2-\xi\frac{1+\nu}{2}D\varphi_{y2,y}=0\\
&\left(D-\beta_2 N_L\right)\varphi_{y2,yy}-\left(\kappa Gh+\xi^2\left(D\frac{1-\nu}{2}-\alpha_2 N_L\right)\right)\varphi_{y2}+\kappa Gh w_{2,y}+\xi\frac{1+\nu}{2}D\varphi_{x2,y}=0
\end{aligned} \tag{11b}$$

and:

$$\begin{aligned}
&\left(\kappa Gh-\beta N_L\right)w_{3,yy}-\kappa Gh\varphi_{y3,y}=0\\
&\left(\frac{1-\nu}{2}D-\beta_1 N_L\right)\varphi_{x3,yy}-\kappa Gh\varphi_{x3}+a^{-1}\left(\frac{1+\nu}{2}D\varphi_{y3,y}+\kappa Gh w_3\right)=0\\
&\left(D-\beta_2 N_L\right)\varphi_{y3,yy}+\kappa Gh w_{3,y}-\kappa Gh\varphi_{y3}=0
\end{aligned} \tag{11c}$$

$$\begin{aligned}
&\left(\kappa Gh-\beta N_L\right)w_{4,yy}-\kappa Gh\varphi_{y4,y}-a^{-1}\kappa Gh\varphi_{x4}=0\\
&\left(\frac{1-\nu}{2}D-\beta_1 N_L\right)\varphi_{x4,yy}-\kappa Gh\varphi_{x4}=0\\
&\left(D-\beta_2 N_L\right)\varphi_{y4,yy}+\kappa Gh w_{4,y}-\kappa Gh\varphi_{y4}+D\frac{1+\nu}{2a}\varphi_{x4,y}=0
\end{aligned} \tag{11d}$$

By collecting the displacements and the corresponding derivatives into the symbolic vectors as follows:

$$\begin{aligned}
&\mathbf{w}_{i,y}=\begin{bmatrix} w_{i,yy} & w_{i,y} & \varphi_{xi,yy} & \varphi_{xi,y} & \varphi_{yi,yy} & \varphi_{yi,y}\end{bmatrix}^T,\ i=1...4\\
&\mathbf{w}_{i}=\begin{bmatrix} w_{i,y} & w_{i} & \varphi_{xi,y} & \varphi_{xi} & \varphi_{yi,y} & \varphi_{yi}\end{bmatrix}^T,\ i=1...4
\end{aligned} \tag{12}$$

equations (9) and (10) can be rewritten in the following compact form:

$$\begin{aligned}
&\begin{bmatrix}\mathbf{w}_{1,y}\\ \mathbf{w}_{2,y}\end{bmatrix}-\begin{bmatrix}\mathbf{A}_{11} & \mathbf{A}_{12}\\ \mathbf{A}_{21} & \mathbf{A}_{22}\end{bmatrix}\begin{bmatrix}\mathbf{w}_{1}\\ \mathbf{w}_{2}\end{bmatrix}=\begin{bmatrix}\mathbf{0}\\ \mathbf{0}\end{bmatrix}\\
&\begin{bmatrix}\mathbf{w}_{3,y}\\ \mathbf{w}_{4,y}\end{bmatrix}-\begin{bmatrix}\mathbf{A}_{33} & \mathbf{A}_{34}\\ \mathbf{A}_{43} & \mathbf{A}_{44}\end{bmatrix}\begin{bmatrix}\mathbf{w}_{3}\\ \mathbf{w}_{4}\end{bmatrix}=\begin{bmatrix}\mathbf{0}\\ \mathbf{0}\end{bmatrix}
\end{aligned} \tag{13}$$

In eq. (13) the matrices $\mathbf{A}_{ij}\ \left(i=1,4;\ j=1,4\right)$ have the following representation:

$$\mathbf{A}_{11}=\begin{bmatrix} 0 & a_{1,2} & 0 & a_{1,4} & a_{1,5} & 0 \\ a_{2,1} & 0 & 0 & 0 & 0 & 0 \\ 0 & a_{3,2} & 0 & a_{3,4} & a_{3,5} & 0 \\ 0 & 0 & a_{4,3} & 0 & 0 & 0 \\ a_{5,1} & 0 & a_{5,3} & 0 & 0 & a_{5,6} \\ 0 & 0 & 0 & 0 & a_{6,5} & 0 \end{bmatrix};\ \mathbf{A}_{12}=\begin{bmatrix} a_{1,7} & 0 & 0 & 0 & 0 & 0 \\ 0 & 0 & 0 & 0 & 0 & 0 \\ 0 & 0 & a_{3,9} & 0 & 0 & 0 \\ 0 & 0 & 0 & 0 & 0 & 0 \\ 0 & 0 & 0 & 0 & a_{5,11} & 0 \\ 0 & 0 & 0 & 0 & 0 & 0 \end{bmatrix};$$

$$\mathbf{A}_{21}=\begin{bmatrix} a_{7,1} & 0 & 0 & 0 & 0 & 0 \\ 0 & 0 & 0 & 0 & 0 & 0 \\ 0 & 0 & a_{9,3} & 0 & 0 & 0 \\ 0 & 0 & 0 & 0 & 0 & 0 \\ 0 & 0 & 0 & 0 & a_{11,5} & 0 \\ 0 & 0 & 0 & 0 & 0 & 0 \end{bmatrix};\ \mathbf{A}_{22}=\begin{bmatrix} 0 & a_{7,8} & 0 & a_{7,10} & a_{7,11} & 0 \\ a_{8,7} & 0 & 0 & 0 & 0 & 0 \\ 0 & a_{9,8} & 0 & a_{9,10} & a_{9,11} & 0 \\ 0 & 0 & a_{10,9} & 0 & 0 & 0 \\ a_{11,7} & 0 & a_{11,9} & 0 & 0 & a_{11,12} \\ 0 & 0 & 0 & 0 & a_{12,11} & 0 \end{bmatrix}; \tag{14a}$$

and:

$$\mathbf{A}_{33}=\begin{bmatrix} 0 & 0 & 0 & 0 & a_{13,17} & 0 \\ a_{14,13} & 0 & 0 & 0 & 0 & 0 \\ 0 & 0 & 0 & 0 & 0 & 0 \\ 0 & 0 & a_{16,15} & 0 & 0 & 0 \\ a_{17,13} & 0 & 0 & 0 & 0 & a_{17,18} \\ 0 & 0 & 0 & 0 & a_{18,17} & 0 \end{bmatrix};\ \mathbf{A}_{34}=\begin{bmatrix} 0 & 0 & 0 & 0 & 0 & 0 \\ 0 & 0 & 0 & 0 & 0 & 0 \\ 0 & 0 & 0 & a_{15,22} & 0 & 0 \\ 0 & 0 & 0 & 0 & 0 & 0 \\ 0 & 0 & 0 & 0 & 0 & 0 \\ 0 & 0 & 0 & 0 & 0 & 0 \end{bmatrix};$$

$$\mathbf{A}_{43}=\begin{bmatrix} a_{19,13} & 0 & 0 & 0 & 0 & 0 \\ 0 & 0 & 0 & 0 & 0 & 0 \\ 0 & a_{21,14} & 0 & a_{21,16} & a_{21,17} & 0 \\ 0 & 0 & 0 & 0 & 0 & 0 \\ 0 & 0 & 0 & 0 & a_{23,17} & 0 \\ 0 & 0 & 0 & 0 & 0 & 0 \end{bmatrix};\ \mathbf{A}_{44}=\begin{bmatrix} 0 & 0 & 0 & a_{19,22} & a_{19,23} & 0 \\ a_{20,19} & 0 & 0 & 0 & 0 & 0 \\ 0 & 0 & a_{21,21} & 0 & 0 & 0 \\ 0 & 0 & a_{22,21} & 0 & 0 & 0 \\ a_{23,19} & 0 & a_{23,21} & 0 & 0 & a_{23,24} \\ 0 & 0 & 0 & 0 & a_{24,23} & 0 \end{bmatrix}; \tag{15}$$

with non-null terms:

$$\begin{aligned}
&a_{2,1}=a_{4,3}=a_{6,5}=a_{8,7}=a_{10,9}=a_{12,11}=1;\\
&a_{1,2}=\frac{\xi^2\left(\kappa Gh-\alpha N_L\right)}{\kappa Gh-\beta N_L};a_{1,4}=\frac{\xi\kappa Gh}{\beta N_L-\kappa Gh};a_{1,5}=\frac{\kappa Gh}{\kappa Gh-\beta N_L};\ a_{1,7}=\frac{2\xi\gamma N_L}{\beta N_L-\kappa Gh};\\
&a_{3,2}=\frac{-2\xi\kappa Gh}{D\left(1-\nu\right)-2\beta_1 N_L};a_{3,4}=\frac{2\left(\kappa Gh+\xi^2\left(D-\alpha_1 N_L\right)\right)}{D\left(1-\nu\right)-2\beta_1 N_L};a_{3,5}=\frac{-\xi D\left(1+\nu\right)}{D\left(1-\nu\right)-2\beta_1 N_L};\\
&a_{3,9}=\frac{4\xi\gamma_1 N_L}{D\left(1-\nu\right)-2\beta_1 N_L};a_{5,1}=\frac{-\kappa Gh}{D-\beta_2 N_L};a_{5,3}=\frac{\xi D\left(1+\nu\right)}{2\left(D-\beta_2 N_L\right)};a_{5,11}=\frac{-2\xi\gamma_2 N_L}{D-\beta_2 N_L};\\
&a_{7,1}=\frac{2\xi\gamma N_L}{\kappa Gh-\beta N_L};a_{7,8}=\frac{\xi^2\left(\kappa Gh-\alpha N_L\right)}{\kappa Gh-\beta N_L};a_{7,10}=\frac{\xi\kappa Gh}{\kappa Gh-\beta N_L};a_{7,11}=\frac{\kappa Gh}{\kappa Gh-\beta N_L};\\
&a_{9,3}=\frac{-4\xi\gamma_1 N_L}{D\left(1-\nu\right)-2\beta_1 N_L};a_{9,8}=\frac{2\xi\kappa Gh}{D\left(1-\nu\right)-2\beta_1 N_L};a_{9,10}=\frac{2\left(\kappa Gh+\xi^2\left(D-\alpha_1 N_L\right)\right)}{D\left(1-\nu\right)-2\beta_1 N_L};\\
&a_{9,11}=\frac{\xi D\left(1+\nu\right)}{D\left(1-\nu\right)-2\beta_1 N_L};a_{5,6}=\frac{2\kappa Gh+\xi^2\left(D\left(1-\nu\right)-2\alpha_2 N_L\right)}{2\left(D-\beta_2 N_L\right)};a_{11,5}=\frac{2\xi\gamma_2 N_L}{D-\beta_2 N_L};\\
&a_{11,7}=\frac{-\kappa Gh}{D-\beta_2 N_L};a_{11,9}=\frac{-\xi D\left(1+\nu\right)}{2\left(D-\beta_2 N_L\right)};a_{11,12}=\frac{2\kappa Gh+\xi^2\left(D\left(1-\nu\right)-2\alpha_2 N_L\right)}{2\left(D-\beta_2 N_L\right)};
\end{aligned}\tag{16}$$

and:

$$\begin{aligned}
&a_{14,13}=a_{16,15}=a_{18,17}=a_{20,19}=a_{22,21}=a_{24,23}=1;\\
&a_{13,17}=\frac{\kappa Gh}{\kappa Gh-\beta N_L};a_{15,22}=\frac{2\kappa Gh}{D\left(1-\nu\right)-2\beta_1 N_L};a_{17,13}=\frac{-\kappa Gh}{D-\beta_2 N_L};a_{17,18}=\frac{\kappa Gh}{D-\beta_2 N_L};\\
&a_{19,13}=\frac{2\gamma N_L}{a\left(\kappa Gh-\beta N_L\right)};a_{19,22}=\frac{\kappa Gh}{a\left(\kappa Gh-\beta N_L\right)};a_{19,23}=\frac{\kappa Gh}{\kappa Gh-\beta N_L};a_{23,17}=\frac{2\gamma_2 N_L}{a\left(D-\beta_2 N_L\right)};\\
&a_{21,16}=\frac{2\kappa Gh}{D\left(1-\nu\right)-2\beta_1 N_L};a_{21,17}=\frac{-D\left(1+\nu\right)}{a\left(D\left(1-\nu\right)-2\beta_1 N_L\right)};a_{21,21}=\frac{4\gamma_1 N_L}{a\left(D\left(1-\nu\right)-2\beta_1 N_L\right)};\\
&a_{21,14}=\frac{-2\kappa Gh}{a\left(D\left(1-\nu\right)-2\beta_1 N_L\right)};a_{23,19}=\frac{-\kappa Gh}{D-\beta_2 N_L};a_{23,21}=\frac{-D\left(1+\nu\right)}{2a\left(D-\beta_2 N_L\right)};a_{23,24}=\frac{\kappa Gh}{D-\beta_2 N_L};
\end{aligned}\tag{17}$$

if the following concise forms are introduced:

$$\begin{aligned}
&\mathbf{w}=\begin{bmatrix}\mathbf{w}_1 & \mathbf{w}_2 & \mathbf{w}_3 & \mathbf{w}_4\end{bmatrix}^T;\\
&\mathbf{w},_y=\begin{bmatrix}\mathbf{w}_{1,y} & \mathbf{w}_{2,y} & \mathbf{w}_{3,y} & \mathbf{w}_{4,y}\end{bmatrix}^T;
\end{aligned}\tag{18}$$

and:

$$\mathbf{A}=\begin{bmatrix}\begin{matrix}\mathbf{A}_{11} & \mathbf{A}_{12}\\ \mathbf{A}_{21} & \mathbf{A}_{22}\end{matrix} & \mathbf{0}\\ \mathbf{0} & \begin{matrix}\mathbf{A}_{33} & \mathbf{A}_{43}\\ \mathbf{A}_{34} & \mathbf{A}_{44}\end{matrix}\end{bmatrix}\tag{19}$$

the equation set (13) can be rewritten as:

$$\mathbf{w},_y - \mathbf{A}\cdot\mathbf{w} = \mathbf{0} \tag{20}$$

To solve equation (20) the matrix **A** is reduced to its canonical form:

$$\mathbf{A} = \mathbf{PDP}^{-1} \tag{21}$$

where the matrix **D** is the eigenvalues matrix $\mathbf{D} = diag\left(\lambda_1, \lambda_2, \ldots \lambda_{24}\right)$ of **A**, and $\mathbf{P} = \left[\mathbf{P}_1, \mathbf{P}_2, \ldots \mathbf{P}_{24}\right]$ is the eigenvectors matrix.

Once the eigenproblem of A is solved, the solution of equation (20) can be expressed as follows:

$$\mathbf{w} = \left(\mathbf{P}e^{\mathbf{D}\cdot y}\mathbf{P}^{-1}\right)\cdot\mathbf{c} \tag{22}$$

In equation (22) the exponential matrix:

$$\mathbf{e}^{\mathbf{D}\cdot y} = \begin{bmatrix} e^{\lambda_1\cdot y} & 0 & \cdots & 0 \\ 0 & e^{\lambda_2\cdot y} & \cdots & 0 \\ \vdots & \vdots & \ddots & \vdots \\ 0 & 0 & \cdots & e^{\lambda_{24}\cdot y} \end{bmatrix} \tag{23}$$

has been introduced. The vector:

$$\mathbf{c} = \left[c_1 \cdots c_{24}\right]^T \tag{24}$$

contains 24 constants of integration that have to be determined by imposing the proper boundary conditions.

According to Mindlin's model, the shear force $\left(V_x, V_y\right)$, the bending moment $\left(M_x, M_y\right)$ and the torque M_{xy} distributed on the boundary edge can be defined in terms of displacement derivatives as follows:

$$\begin{aligned} V_x &= -\kappa Gh\left(\varphi_x - w,_x\right) + N_x w,_x + N_{xy} w,_y ; \\ V_y &= -\kappa Gh\left(\varphi_y - w,_y\right) + N_{xy} w,_x + N_y w,_y ; \\ M_x &= -D\left(\varphi_x,_x + \nu\varphi_y,_y\right); \\ M_{xy} &= M_{yx} = -D\frac{1-\nu}{2}\left(\varphi_x,_y + \varphi_y,_x\right) \\ M_y &= -D\left(\varphi_y,_y + \nu\varphi_x,_x\right) \end{aligned} \tag{25}$$

That is, by substituting the displacement defined in eq. (4):

$$
\begin{aligned}
V_x &= \sin\xi x\left(-\kappa Gh\left(\xi w_2+\varphi_{x2}\right)+\xi\alpha N_L w_2-\gamma N_L w_{1,y}\right)+\\
&\quad \cos\xi x\left(\kappa Gh\left(\xi w_1-\varphi_{x1}\right)-\xi\alpha N_L w_1-\gamma N_L w_{2,y}\right)-\\
&\quad \frac{x}{a}\left(\kappa Gh\varphi_{x4}+\gamma N_L w_{3,y}\right)-\left(\kappa Gh\left(\varphi_{x3}-\frac{w_{3,y}}{a}\right)+\frac{\alpha N_L w_3}{a}+\gamma N_L w_{4,y}\right)\\
V_y &= \sin\xi x\left(\kappa Gh\left(w_{1,y}-\varphi_{y1}\right)+\xi\gamma N_L w_2-\beta N_L w_{1,y}\right)+\\
&\quad \cos\xi x\left(\kappa Gh\left(w_{2,y}-\varphi_{y2}\right)-\xi\gamma N_L w_1-\beta N_L w_{2,y}\right)-\\
&\quad \frac{x}{a}\left(\kappa Gh\left(\varphi_{y3}-w_{3,y}\right)+\beta N_L w_{3,y}\right)-\left(\kappa Gh\left(\varphi_{y4}-w_{4,y}\right)+\frac{\gamma N_L w_3}{a}+\beta N_L w_{4,y}\right)
\end{aligned}
\tag{26}
$$

and:

$$
\begin{aligned}
M_x &= D\left(\sin\xi x\left(\xi\varphi_{x1}-\nu\varphi_{y1,y}\right)-\cos\xi x\left(\xi\varphi_{x2}+\nu\varphi_{y2,y}\right)-\frac{x}{a}\nu\varphi_{y3,y}-\left(\frac{\varphi_{x4}}{a}+\nu\varphi_{x4,y}\right)\right)\\
M_y &= D\left(\sin\xi x\left(\xi\nu\varphi_{x1}-\varphi_{y1,y}\right)-\cos\xi x\left(\xi\nu\varphi_{x2}+\varphi_{y2,y}\right)-\frac{x}{a}\varphi_{y3,y}-\left(\frac{\nu\varphi_{x4}}{a}+\varphi_{x4,y}\right)\right)\\
M_{xy} &= D\frac{1-\nu}{2}\left(\sin\xi x\left(\xi\varphi_{y2}-\varphi_{x2,y}\right)-\cos\xi x\left(\xi\varphi_{y1}+\varphi_{x1,y}\right)-\frac{x}{a}\varphi_{y4,y}-\left(\frac{\varphi_{y3}}{a}+\varphi_{x3,y}\right)\right)
\end{aligned}
\tag{27}
$$

Eqns. (26) and (27) allow the complementary conditions along the plate's boundaries to be set in either essential or natural case (i.e. Dirichlet or Neumann ones):

$$
\begin{aligned}
&w=0 \quad \text{or } V_x=0\\
&\varphi_x=0 \ \text{ or } M_x=0\\
&\varphi_y=0 \ \text{ or } M_{xy}=0
\end{aligned}
\tag{28}
$$

at $x=\pm a/2$, and:

$$
\begin{aligned}
&w=0 \quad \text{or } V_y=0\\
&\varphi_x=0 \ \text{ or } M_{xy}=0\\
&\varphi_y=0 \ \text{ or } M_y=0
\end{aligned}
\tag{29}
$$

at $y=\pm b/2$.

The boundary conditions (28) and (29) can be finally used to evaluate the 24 constants of integration **c** in eq. (24). In order to match the unknown, the boundary conditions (28) and (29) have to be collocated in eight different boundary points. By considering the $\left(P_1 ... P_8\right)$ points depicted in Figure 3, the solution is numerically defined on the four horizontal lines $\left(a_1,a_2,a_3,a_4\right)$:

$$
\begin{aligned}
\mathbf{w}(a_1) &= \mathbf{w}(y=b/2) = \left(\mathbf{P}e^{\mathbf{D}\cdot(b/2)}\mathbf{P}^{-1}\right)\cdot\mathbf{c} \\
\mathbf{w}(a_2) &= \mathbf{w}(y=-b/2) = \left(\mathbf{P}e^{\mathbf{D}\cdot(-b/2)}\mathbf{P}^{-1}\right)\cdot\mathbf{c} \\
\mathbf{w}(a_3) &= \mathbf{w}(y=b/4) = \left(\mathbf{P}e^{\mathbf{D}\cdot(b/4)}\mathbf{P}^{-1}\right)\cdot\mathbf{c} \\
\mathbf{w}(a_4) &= \mathbf{w}(y=-b/4) = \left(\mathbf{P}e^{\mathbf{D}\cdot(-b/4)}\mathbf{P}^{-1}\right)\cdot\mathbf{c}
\end{aligned}
\tag{30}
$$

so that the eight equations containing the nodal values of w in terms of the constant **c** can be obtained as follows:

$$
\begin{aligned}
w_{P_1} &= \left(w\left(x=\frac{a}{4}, y=\frac{b}{2}\right)\right) = w_1(a_1)\cdot\sin\left(\frac{m\pi}{4}\right) + w_2(a_1)\cdot\cos\left(\frac{m\pi}{4}\right) + w_3(a_1)\cdot\left(\frac{1}{4}\right) + w_4(a_1) \\
&\vdots \\
w_{P_8} &= \left(w\left(x=-\frac{a}{2}, y=-\frac{b}{4}\right)\right) = -w_1(a_4)\cdot\sin\left(\frac{m\pi}{2}\right) + w_2(a_4)\cdot\cos\left(\frac{m\pi}{2}\right) - w_3(a_4)\cdot\left(\frac{1}{2}\right) + w_4(a_4)
\end{aligned}
\tag{31}
$$

In a similar way it is possible to define any kinematic and static variables reported in eqns. (28) and (29) in terms of the integration constants **c**. Finally, the applied boundary conditions lead to an homogeneous linear algebraic system:

$$
\mathbf{G}\cdot\mathbf{c} = \mathbf{0} \tag{32}
$$

of 24 equations in 24 unknowns. The nontrivial solution is found by setting the determinant of **G** equal to zero. Given the dependence of the matrix **G** by the axial load N_L, the determinant vanishes when the axial load reaches the critical value N_{cr}. However, a non-linear equation is provided as the elements a_{ij} of the matrix **A** are related to the applied load N_L, and a bisection algorithm is proposed in the present paper as converging in a few steps. It can be summarized as follows:

1) Assign an initial, small value of N_{cr}, an increment ΔN_{cr} and an error tolerance e (in the examples $N_{cr} = 0$, $\Delta N_{cr} = 10$ and $e = 0.000001$).

2) By means of N_{cr} and ΔN_{cr}, compute the matrix **A** (eq. (19)), its eigenvalues and eigenvectors **P**, **D** (eq. (21)) and, finally, the exponential matrices $\mathbf{e}^{D\cdot y}$ on the nodal lines (a_1, a_2) and (a_3, a_4) by considering, in eq. (25), the values $y = \pm a/2$ and $y = \pm a/4$, respectively.

3) Compute the nodal forces and displacement (eq. 30).

4) Check: If $sign\left(\det\mathbf{G}(N_{cr})\right) = sign\left(\det\mathbf{G}(N_{cr} + \Delta N_{cr})\right)$, consider a new $N_{cr} = N_{cr} + \Delta N_{cr}$ and go back to the step 2). If $sign\left(\det\mathbf{G}(N_{cr})\right) \neq sign\left(\det\mathbf{G}(N_{cr} + \Delta N_{cr})\right)$, consider a new $\Delta N_{cr} = \Delta N_{cr}/2$ and go to next step.

5) If $\Delta N_{cr} < e$, stop the iteration, otherwise return to step 2.

It is worth noticing that the analytical approach of the proposed method provides results that do not depend on the adopted discretization. Furthermore, the eigenvalue problem can be performed on a single element in order to provide reliable results, thus the 24 constants of the vector c are the highest number of unknowns that can be involved and no refinement is required. C2

3 RESULTS

The results achieved by using the proposed solution have been compared to the ones depicted in Liew *et al.* [10], Ruocco [14], Mizusawa [21], Shufrin and Eisenberger [22], Yang *et al.* [23], Hosseini-Hashemi *et al.* [24], Xiang [25], Bui *et al.* [26] and Vrcelj and Bradford [27]. Six different boundary conditions have been considered in the tests. For the sake of simplicity, capital letters shall denote the boundary conditions at each side of the plate, that is C stands for clamped supported, S for Simply supported, F for Free. For instance, the string S-S-S-S means that the plate is simply-supported on all four edges while, the string S-F-S-F indicates a plate with alternate simply-supported and free sides. The acting loads are indicated by the load coefficients (α, β, γ), namely with $(\alpha = 1, \beta = \gamma = 0)$ we indicate load acting in *x*-direction, with $(\alpha = \gamma = 0, \beta = 1)$ a load acting in *y*-direction, with $(\alpha = \beta = 1, \gamma = 0)$ equal biaxial loads acting in both *x*- and *y*-direction and so on.

In the proposed examples, a Poisson ratio $\nu = 0.3$ and a shear correction factor $\kappa = \frac{5}{6}$ have been considered. The buckling load is reported in the following dimensionless form:

$$\eta_{cr} = N_{cr} a^2 / \pi^2 D \tag{33}$$

Tables 1, 2 and 3 report the results for thin $(\delta / a = 0.05)$, moderately thick $(\delta / a = 0.1)$ and thick $(\delta / a = 0.2)$ plates subjected to uniaxial and biaxial load conditions, and for different boundary conditions. Although the procedure is highly sensitive for plates with relatively small thickness ratios, the comparison of the results shows an excellent agreement between the proposed solution and those available in the literature.

Both the Von Kármán strain model ($k_1 = k_2 = 0$ in eq. (6), depicted with “Present (a)” in the tables) and the Koiter-Sanders strain model ($k_1 = k_2 = 1$ in eq. (6), depicted with “Present (b)” in the tables) have been tested. As it was to be expected, the Koiter-Sanders strain model provides a critical load lower than the critical load achieved by adopting the Von Kármán strain model. However, the magnitude of the difference (never greater than 3%) validates the usual adoption of the simple Von Kármán model for plate plates and common load conditions.

Table 4 compares the shear buckling factor obtained with the present formulation for square plates with two different boundary conditions with some analytical [1] and numerical [24,25] solutions available in the literature. The comparison shows again a good agreement, although the presented solution returns lower magnitude of the critical load in all the proposed example. It is worth noting that the analytical solution reported in literature is obtained in the Kirchhoff thin plate theory, and should not match the Mindlin model for moderately thick plates.

In table 5 we present the critical buckling factor for a thick C-C-C-C square plate with thickness-to-width ratio $\delta / a = 0.1$ and $\delta / a = 0.15$, respectively. A different magnitude of the compressive load in *x*- and *y*-direction, that is $\alpha = 1.5$ and $\beta = 1$ in eq. 7 is also considered. The obtained results have been compared with ones published in Bui *et al.* [26] (in which the analysis is based on a shear-locking-free and mesh-free method) and with the Finite element results in Yang *et al.* [23].

The critical parameter obtained analytically with the proposed method is slightly lower than the results available in literature when the Von Kármán strain measure is considered (Present (a) in the table). The adoption of the Koiter-Sanders strain measure further reduces the results.

Finally, the results reported in Table 6 show the influence of the choice of the position of the eight points $\left(P_1 ... P_8\right)$ on the response of S-S-S-S Mindlin plates subjected to an equal biaxial in-plane load (Figure 4). It is possible to say that the critical load does not depend on the position of the representative points. Only when $\beta_1 = -\beta_2 = 1/2$, for any value of α_1, α_2 the solution does not converge: such cases produce a linear combination of displacement and force vectors required for the **G** matrix, and the numerical analysis returns a determinant close to zero for any value of N_{cr}.

4 CONCLUSION

In the present paper a closed-form solution for studying the critical behavior of rectangular, moderately thick, plates without any use of approximation on the boundary conditions has been presented. The model is based on the extended Kantorovich method and performs a decoupling of variables with respect to two orthogonal coordinate directions, namely *x*- and *y*-direction. To the best of author's knowledge, this is the first application of the procedure to the Mindlin plate analysis. Some numerical results have been reported and compared with analytical and numerical values available in the literature. Although only regular plates are considered in this paper, the method can be extended, through a finite element procedure and adopting the closed form solution proposed in the paper as shape functions, to plates with more complex geometries, or for analysis of anisotropic plates.

REFERENCES

[1] Timoshenko S.P. and Gere J.M., *Theory of elastic stability*, (3rd ed.)McGraw-Hill, New York, 1970.

[2] Wang X. and Wang Y., A differential quadrature analysis of vibration and buckling of an SS-C-SS-C rectangular plate loaded by linearly varying in-plane stresses, *Journal of Sound and Vibration* 298(1), 420-431, 2006

[3] Kobayashi H. and Sonoda K., Vibration and buckling of tapered rectangular plates with two opposite edges simply supported and the other two edges elastically restrained against rotation, *Journal of Sound and Vibration* 146, 323-337, 1991.

[4] Leissa A.W. and Kang J.H., Exact solution for vibration and buckling of an SS-C-SS-C rectangular plate loaded by linearly varying in-plane stresses, *International Journal of Mechanical Sciences* 44, 1925-45, 2002.

[5] Ruocco E. and Mallardo V., “Buckling analysis of Levy-type orthotropic stiffened plate and shells based on different strain-displacement models”, *International Journal of Non-Linear Mechanics* 50, 40-47, 2013.

[6] Reddy J.N., A general non-linear third order theory of plates with moderate thickness, *International Journal of Non-Linear Mechanics* 25, 677-686, 1990.

[7] Sayyad A.S. and Ghugal Y.M., On the buckling of isotropic, transversely isotropic and laminated composite rectangular plates, *International Journal of Structural Stability and Dynamics* 14(7), 1-32, 2014.

[8] Hong G.M., Wang C.M. and Tan T.J., Analytical buckling solutions for circular Mindlin plates: inclusion of inplane prebuckling deformation, *Archive of Applied Mechanics* 63(8), 534-542, 1993.

[9] Wang C.M., Wang C.Y. and Reddy J.N, *Exact solutions for buckling of structural members,* CRC press, Boca Raton, Florida, 2004.

[10] Liew K.M., Xiang Y. and Kitipornchai S., Analytical buckling solutions for Mindlin plates involving free edges, International Journal of Mechanical Sciences, 38(10), 1127–1138, 1996.

[11] Xiang Y., Wei G.W., Exact solution for buckling and vibration of stepped rectangular Mindlin plates, International Journal of Solids and Structures, 41, 279–294, 2004.

[12] Hosseini-Hashemi S. and Arsanjani M., Exact characteristic equations for some of classical boundary conditions of vibrating moderately thick rectangular plates, International Journal of Solids and Structures, 42, 819-853, 2005.

[13] Ruocco E. and Minutolo V., Buckling analysis of Mindlin plates undred the Green-Lagrange strain hypothesis, International Journal of Structural Stability and Dynamics 15(6), 1-29, 2014.

[14] Ruocco E., Effect of nonlinear strain components on the buckling response of stiffened shear-deformable composite plates, Composite: Part B 69, 31-43, 2015.

[15] Abolghasemia S., Eipakchi H. and Shariatib M., An analytical solution for axisymmetric buckling of annular plates based on perturbation technique, Int J Mech Sci 123, 74-83, 2017.

[16] Van Dung D. and Quan Chan D., Analytical investigation on mechanical buckling of FGM truncated conical shells reinforced by orthogonal stiffeners based on FSDT, Composite Structures 159, 827-841, 2017.

[17] Canales F.G. and Mantari J.L., Buckling and free vibration of laminated beams with arbitrary boundary conditions using a refined HSDT, Composites Part B: Engineering 100, 136-145, 2016.

[18] Huu-tai Thai and Dong-Ho Choi, Analytical solutions of refined plate theory for bending, buckling and vibration analyses of thick plates, Applied Mathematical Modelling 37(18-19), 8310-8321, 2013.

[19] Ruocco E. and Minutolo V., Buckling of composite plates with arbitrary boundary conditions by a semianalytical approach, International Journal of Structural Stability and Dynamics 12(5), 1-16, 2012.

[20] Ruocco E., Minutolo V. and Ciaramella S. A generalized analytical approach for the buckling analysis of thin rectangular plates with arbitrary boundary condition, International Journal of Structural Stability and Dynamics 11(1), 1-21, 2011.

[21] Mizusawa T., Buckling of rectangular Mindlin plates with tapered thickness by the spline strip method, International Journal of Solids and Structures 30, 1663–1677, 1993.

[22] Shufrin I. and Eisenberger M., Stability and vibration of shear deformable plates—first order and higher order analyses, International Journal of Solids and Structures 42, 1225–1251, 2005.

[23] Yang Z., Chen X., Zhang X. and He Z., Free vibration and buckling analysis of plates using B-spline wavelet in the interval Mindlin element, Applied Mathematical Modelling 37, 3449-3466, 2013.

[24] Hosseini-Hashemi S., Khorshidi K. and Amabili M., Exact solution for linear buckling of rectangular Mindlin plates, Journal of Sound and Vibration, 315, 318–342, 2008.

[25] Xiang Y., Numerical Developments in Solving the Buckling and Vibration of Mindlin Plates, PhD Thesis, The University of Queensland, Australia, 1993.

[26] Bui T.Q., Nguyen M.N. and Zhang C., Buckling analysis of Reissner–Mindlin plates subjected to in-plane edge loads using a shear-locking-free and meshfree method, Engineering Analysis with Boundary Elements 35, 1038-1053, 2011.

[27] Vrcelj Z. and Bradford M.A., A simple method for the inclusion of external and internal supports in the spline finite strip method (SFSM) of buckling analysis, Computers and Structures 86, 529-544, 2008.

List of figures

Figure 1: Reference system and load condition
Figure 2: The assumed displacement field
Figure 3: The chosen points for applying the boundary conditions
Figure 4: Different coordinate for the points chosen for imposing the boundary conditions.

Figure 1: Reference system and load condition

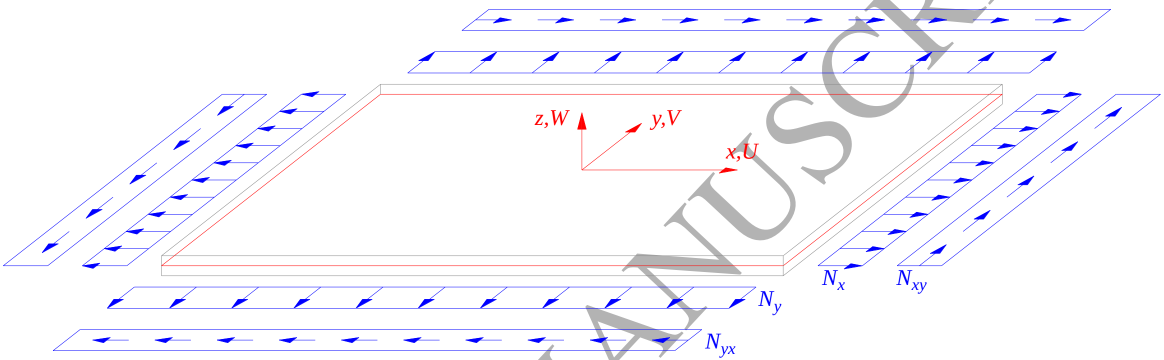

Figure 2: The assumed displacement field

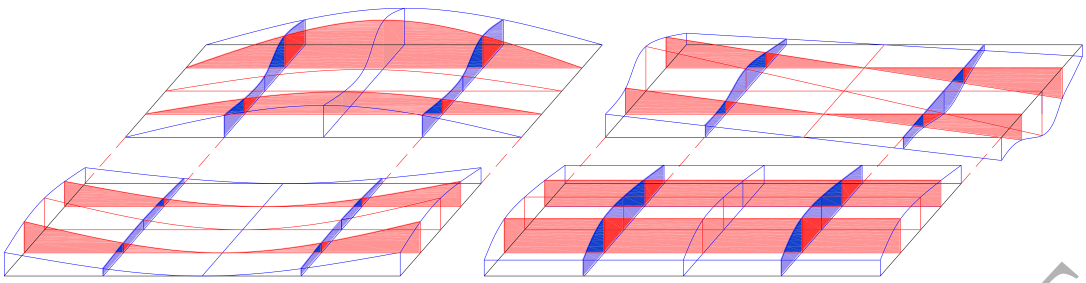

Figure 3: The chosen points for applying the boundary conditions

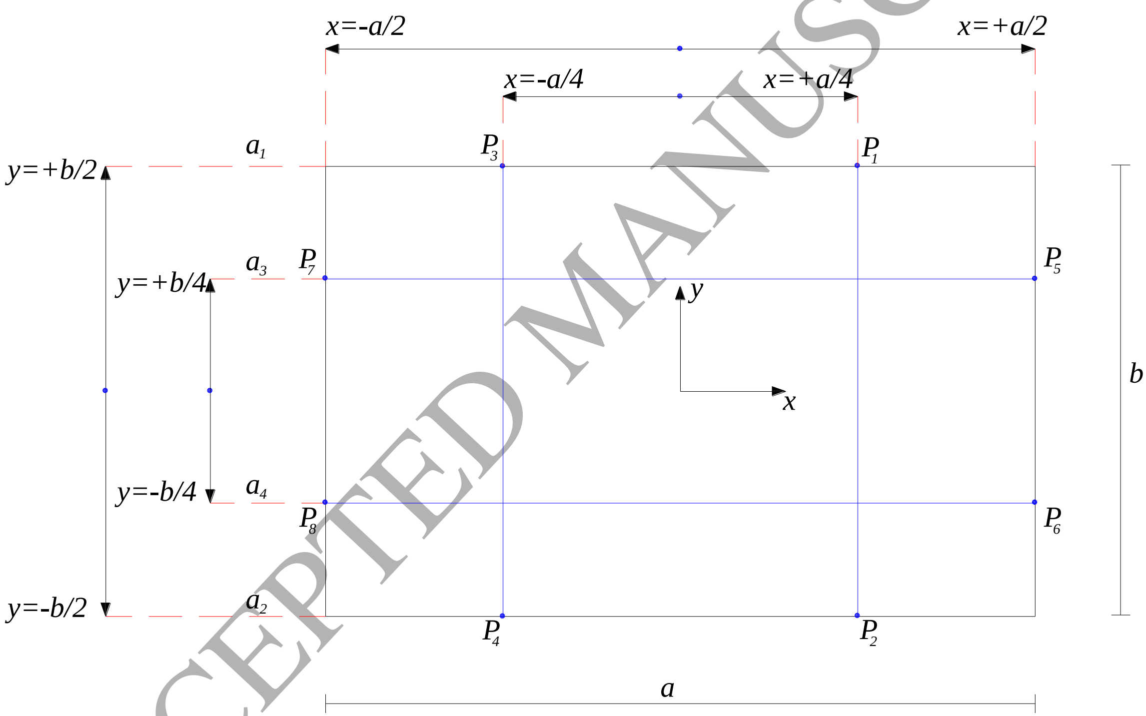

Figure 4: Different coordinate for the points chosen for imposing the boundary conditions.

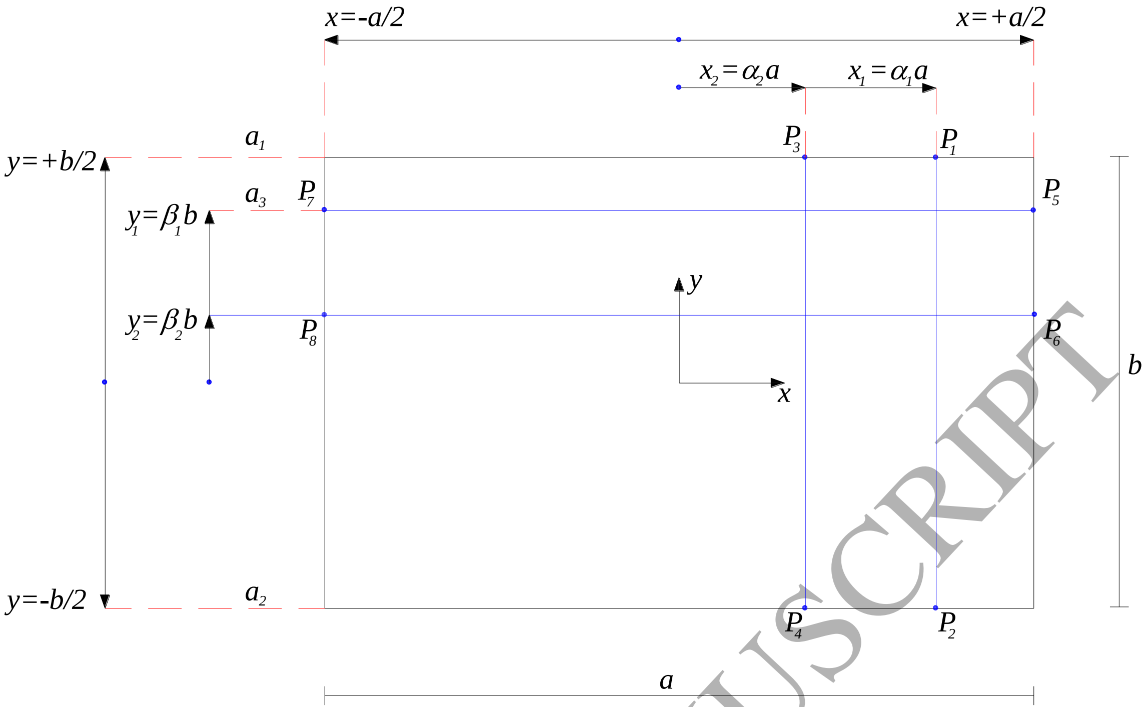

Table 1: Buckling factor η_{cr} for square plates subjected to monoaxial in-plane load in *x* direction (α=1, β=γ=0).

Boundary Conditions	Method	δ/a		
		0.05	0.1	0.2
S-S-S-S	Mizusawa [16]	3.9440	3.7290	3.2560
	Shufrin and Eisenberger [17]	-	3.7865	3.2637
	Yang *et al.* [18]	3.9327	3.7352	3.1287
	Ruocco and Minutolo [15]	3.9444	3.7865	3.2637
	Present (Von Karman)	3.9501	3.7865	3.2637
	Present (Koiter-Sanders)	3.9168	3.7314	3.1255
S-C-S-C	Mizusawa [16]	7.2280	6.370	4.320
	Hosseini-Ashemi et al. [19]	7.2989	6.3698	4.3204
	Ruocco and Minutolo [15]	8.2637	7.4074	5.3190
	Present (Von Karman)	8.2654	7.4074	5.3192
	Present (Koiter-Sanders)	8.2291	7.3011	5.1323
S-C-S-S	Mizusawa [16]	5.5740	5.1400	3.876
	Hosseini-Ashemi et al. [19]	5.5977	5.2171	4.1364
	Ruocco and Minutolo [15]	5.5995	5.2231	4.1509
	Present (Von Karman)	5.6003	5.2232	4.1509
	Present (Koiter-Sanders)	5.5576	5.1458	3.9854
S-C-S-F	Mizusawa [16]	1.6200	1.5560	1.370
	Hosseini-Ashemi et al. [19]	1.6197	1.5558	1.3701
	Ruocco and Minutolo [15]	1.6200	1.5568	1.3727
	Present (Von Karman)	1.6229	1.5568	1.3727
	Present (Koiter-Sanders)	1.6219	1.5403	1.3252
S-F-S-F	Mizusawa [16]	0.9412	0.9146	0.8274
	Shufrin and Eisenberger [17]	0.9433	0.9222	0.8512
	Hosseini-Ashemi et al. [19]	0.9432	0.9222	0.85124
	Ruocco and Minutolo [15]	0.9432	0.9222	0.85124
	Present (Von Karman)	0.9747	0.9222	0.85124
	Present (Koiter-Sanders)	0.9737	0.9149	0.82842

Table 2: Buckling factor η_{cr} for square plates subjected to monoaxial in-plane load in *y* direction (β=1, α=γ=0).

Boundary Conditions	Method	δ/*a*		
		0.05	0.1	0.2
S-S-S-S	Mizusawa [16] Shufrin and Eisenberger [17] Hosseini-Ashemi et al. [19] Present (Von Karman) Present (Koiter-Sanders)	3.928 nc 3.9437 3.9335 3.9332	3.729 3.7865 3.78645 3.78645 3.73141	3.119 3.2637 3.2637 3.2637 3.1255
S-C-S-C	Mizusawa [16] Hosseini-Ashemi et al. [19] Ruocco and Minutolo [15] Present (Von Karman) Present (Koiter-Sanders)	6.462 6.5238 6.5238 6.5262 6.4622	5.765 5.9487 5.9487 5.9578 5.7730	4.109 4.4004 4.4207 4.4207 4.1863
S-C-S-S	Mizusawa [16] Hosseini-Ashemi et al. [19] Present (Von Karman) Present (Koiter-Sanders)	4.717 4.7454 4.7455 4.7227	4.372 4.4656 4.4701 4.3766	3.418 3.6115 3.6237 3.1364
S-C-S-F	Mizusawa [16] Liew et al. [10] Hosseini-Ashemi et al. [19] Ruocco and Minutolo [15] Present (Von Karman) Present (Koiter-Sanders)	2.260 2.2667 2.2667 2.2667 1.9901 2.2613	2.078 2.1010 2.1010 2.1032 2.1033 2.067	1.657 - 1.720 1.722 1.725 1.646
S-F-S-F	Mizusawa [16] Liew et al [10] Shufrin and Eisenberger [17] Hosseini-Ashemi et al. [19] Ruocco and Minutolo [15] Present (Von Karman) Present (Koiter-Sanders)	1.942 1.9456 1.9469 1.9464 1.9464 - 1.5933	1.807 1.8216 1.8234 1.8234 1.8234 1.8234 1.7980	1.497 - 1.5372 1.5372 1.5372 1.5372 1.4765

Table 3: Buckling factor η_{cr} for square plates subjected to equal biaxial in-plane load in *x* and *y* direction (α=β=1, γ=0).

Boundary Conditions	Method	δ/a		
		0.05	0.1	0.2
S-S-S-S	Xiang [20]	1.9719	1.8920	1.7723
	Hosseini-Ashemi et al.[19]	1.9718	1.8919	1.7722
	Ruocco and Minutolo [15]	1.9721	1.8932	1.6318
	Present (Von Karman)	1.9805	1.8932	1.6318
	Present (Koiter-Sanders)	1.9639	1.8657	1.5627
S-C-S-F	Liew et al. [10]	1.1119	1.0641	1.0049
	Hosseini-Ashemi et al. [19]	1.1119	1.0641	1.0049
	Ruocco and Minutolo [15]	1.1119	1.0641	0.9390
	Present (Von Karman)	1.1016	1.0641	0.9390
	Present (Koiter-Sanders)	1.1100	1.0493	0.8967
S-S-S-F	Liew et al. [10]	1.0323	0.9954	0.9476
	Hosseini-Ashemi et al.[19]	1.0322	0.9954	0.9476
	Ruocco and Minutolo [15]	1.0323	0.9954	0.8923
	Present (Von Karman)	1.0437	0.9954	0.8923
	Present (Koiter-Sanders)	1.0229	0.9830	0.8551
S-F-S-F	Shufrin and Eisenberger [17]	0.9208	0.8977	0.8650
	Liew et al. [10]	0.9207	0.8977	0.8651
	Hosseini-Ashemi et al. [19]	0.9207	0.8977	0.8651
	Ruocco and Minutolo [15]	0.9207	0.8977	0.8248
	Present (Von Karman)	-	0.8977	0.8248
	Present (Koiter-Sanders)	0.8992	0.8888	0.7962

Table 4: Buckling factor η_{cr} for square plates subjected to shear load (γ=1, α=β=0).

Boundary Conditions	Present (Von Karman)	Present (Koiter-Sanders)	Timoshenko and Gere [1]	Bui *et al.* [21]	Vrcelj and Bradford [22]
S-S-S-S	9.2689	9.1112	9.33	9.378	9.3847
S-C-S-C	12. 5677	12. 2883	12.58	12.6072	12.5997

Table 5: critical buckling factor η_{cr} for CCCC square plates with two different thickness-to-width ratio δ/a subjected to unequal biaxial in-plane load (α=1.5, β=1, γ=0).

δ/a	Method	η_{cr}
0.1	Bui *et al.* [21]	3.5289
	Yang *et al.* [18]	3.5293
	Present (Von Karman)	3.1850
	Present (Koiter-Sanders)	3.0487
0.15	Bui *et al.* [21]	2.9546
	Yang *et al.* [18]	2.9866
	Present (Von Karman)	2.7137
	Present (Koiter-Sanders)	2.5001

Table 6: Buckling factor for square plates having different position of the representative boundary nodes and subjected to equal biaxial in-plane load.

δ/a	α_1	α_2	β_1	β_2	η_{cr}
0.1	1/100	-1/100	1/100	-1/100	1.8932
	1/100	-1/100	1/4	-1/4	1.8932
	1/100	-1/25	1/45	1/64	1.8932
	1/4	-1/4	1/100	-1/100	1.8932
	1/2	-1/2	1/4	-1/4	1.8932
	1/2	-1/2	1/100	-1/100	1.8932
	α_1	α_2	1/2	-1/2	nc
	1/100	-1/100	1/2	0	1.8932
	1/100	-1/100	1/2-1/100	-1/2+1/100	1.8932